Journal of Nanophotonics

SPIEDigitalLibrary.org/jnp

Noncontact optical metrologies for Young's modulus measurements of nanoporous low-k dielectric thin films

Brian C. Daly
Sheldon T. Bailey
Ratnasingham Sooryakumar
Sean W. King

SPIE

Noncontact optical metrologies for Young's modulus measurements of nanoporous low-k dielectric thin films

Brian C. Daly,[a] Sheldon T. Bailey,[b] Ratnasingham Sooryakumar,[b] and Sean W. King[c]

[a]Vassar College, Department of Physics and Astronomy, 124 Raymond Avenue, Poughkeepsie, New York 12604

[b]Ohio State University, Department of Physics, 191 West Woodruff Avenue, Columbus, Ohio 43210

[c]Intel Corporation, Logic Technology Development, 5200 NE Elam Young Parkway, Hillsboro, Oregon 97124

sean.king@intel.com

Abstract. Brillouin light scattering (BLS) and picosecond laser ultrasonics (PLU) are two noncontact optical techniques that have garnered significant interest for thin film elastic constant measurements. PLU and BLS measurements were utilized to determine the elastic constants of 100 to 500 nm thick nanoporous low-k dielectric materials of significant interest for reducing capacitive delays in nanoelectronic interconnect circuits. PLU measurements with and without a metal acousto-optic transducer are described in detail and compared to previously reported BLS measurements. The values of Young's modulus determined by both BLS and PLU were found to be in excellent agreement and consistent with nanoindentation measurements on thicker 2 micrometer films. While successful BLS measurements were achieved for films as thin as 100 nm, PLU measurements were limited to $> \sim 200$ nm thick films due to experimental constraints on observing acoustic pulses in thinner films. However, these results clearly demonstrate the capability of both BLS and PLU to determine the elastic constants of low-k dielectric materials at the desired thickness targets for future nanoelectronic interconnect technologies. © *2013 Society of Photo-Optical Instrumentation Engineers (SPIE)* [DOI: 10.1117/1.JNP.7.073094]

Keywords: Brillouin light scattering; picosecond laser ultrasonics; Young's modulus; low-k dielectric.

Paper 13007P received Jan. 31, 2013; revised manuscript received Mar. 29, 2013; accepted for publication Apr. 2, 2013; published online Apr. 24, 2013.

1 Introduction

The recent implementation of hi-k gate dielectrics[1] and three-dimensional multi-gate transistors[2] by Intel Corporation has provided a path to continued improvements in transistor performance and density scaling that should enable Moore's law[3] to be maintained for at least another decade.[4] However, in order for the transistor improvements to be manifested in high performance products, additional improvements in the speed of the transistor interconnect system are also needed.[5] For this reason, the semiconductor industry a decade ago made the transition from Al to Cu[6] to lower metal interconnect resistivity and from SiO_2 to silicon oxyfluoride (SiOF)[7] materials to lower dielectric constant and the effective capacitance of the interlayer dielectric (ILD).[8] These moves combined helped to reduce resistance-capacitance (RC) delays in the metal interconnect and avoided having the metal interconnect become the rate limiting speed path.[5] However, due to the lack of metals with significantly lower resistance, continued reductions in RC delays have been primarily achieved by implementing materials with increasingly lower dielectric constants.[9,10]

0091-3286/2013/$25.00 © 2013 SPIE

Beyond SiOF, the next generation of lower dielectric constant (i.e., low-k) materials adopted were inorganic SiOC:H dielectrics[11] with k values ranging from 3.3 to 3.0.[12] These materials consist of an SiO_2 network that is disrupted by the insertion of terminal organic groups (typically CH_3).[9,12] The addition of the terminal organic groups disrupts the SiO_2 network bonding resulting in a material with lower density/more free volume. The increase in free volume (with a dielectric constant by definition = 1) results in a material with an effectively lower dielectric constant due to volume averaging of the dielectric constant of the free volume with the dielectric constant of the SiO_2 network (k = 4). The addition of free volume/decreased network connectivity, however, results in many of the thermal and mechanical properties of these materials being significantly reduced.[9–15] The reduction in these properties has created numerous thermal-mechanical reliability risks for products incorporating low-k materials related to cracking and delamination in the low-k/Cu interconnect during interconnect fabrication, packaging, and operation.[16–18]

Continued reductions in dielectric constant have been achieved via further optimization of the deposition precursors, film composition, and processing conditions. SiOC:H materials with k = 2.55 to 2.7 are now widely utilized in the industry.[19] However, further reduction in dielectric constant below k = 2.5 results in materials with larger free volume and pore sizes approaching 1 nm.[20] This leads to further reductions in the thermal-mechanical properties of these low-k materials.[21] More importantly though, the free volume/porosity present in low-k materials starts to become increasingly interconnected as k drops below 2.5 to 2.7 (the exact k value at which the transition occurs depends on the precursor and processing conditions utilized to deposit the material).[22]

At k < 2.5, significantly interconnected porosity exists in all low-k SiOC:H materials regardless of the precursors and processing conditions. Interconnected porosity represents a significant concern for both low-k/Cu interconnect fabrication and reliability due to the ability of ambient moisture, gaseous precursors, wet chemicals, and metals to easily diffuse through the low-k ILD material.[23,24] The presence of interconnected porosity and the negative effect it has on down-stream patterning and metallization processes needed to fabricate multilayer low-k/Cu interconnects has severely limited the ability of the industry to implement these materials. Accordingly, the date forecasted by the International Technology Roadmap for Semiconductors (ITRS) for insertion of k < 2.5 materials into high volume interconnect manufacturing has been pushed back several years in a row.[25] These difficulties have driven some corporations to consider more complex and/or expensive means for reducing capacitance such as pore stuffing/filling[26] and selective formation of air-gaps between metal lines.[27]

For these reasons, metrologies capable of assessing the mechanical properties of low-k dielectric thin film materials are highly needed. Thin film nanoindentation measurements have proven to be the industry standard technique for assessing mechanical properties such as Young's modulus and fracture toughness.[16] Nanoindentation Young's modulus in particular has become a property of intense focus within the industry due to the speed and simplicity of the measurement and empirical correlations to observed mechanical failures.[16,17] However as the semiconductor industry transitions to <20 nm technologies, thickness targets for low-k ILD materials will start to approach 100 nm.[28] At these thicknesses, nanoindentation Young's modulus measurements on low-k films start to be inflated and dominated by so-called substrate effects that arise due to the higher stiffness of the underlying substrate (typically Si).[29] Replacement metrologies for nanoindentation should therefore be capable of assessing the true mechanical properties of thin film materials in the 10 to 100 nm range and be free of significant substrate effects. Ideally, such replacement techniques would also be noncontact and nondestructive to enable inline testing and monitoring of the mechanical properties of patterned low-k dielectric materials and other nanostructures.

The ability to perform inline testing is highly desirable as the down-stream etching and cleaning processes utilized to fabricate interconnects can significantly damage the low-k material and alter the mechanical properties from their original as deposited values.[30] As the thickness of the damaged area for the low-k dielectric can only be a few nanometers thick, a final requirement for new thin film mechanical property metrologies is the ability to detect and assess the mechanical properties of surface and interfacial layers only a few nanometer thick (additional challenges and

requirements for low-k/Cu interconnect metrologies can be found in the Emerging Research Materials chapter of the 2011 ITRS[25]).

Contact resonance-atomic force microscopy (CR-AFM),[31,32] a technique that relies on detecting shifts in the oscillation frequency of an AFM probe tip as it is brought into and out of contact with the surface of a material, is one approach that has shown potential for measuring the Young's modulus of low-k dielectric thin films[33] and nanometer thick films.[34] Owing to the high spatial resolution capability available with AFM, CR-AFM and related techniques have also been demonstrated capable for assessing the mechanical properties of nanowires[35] and patterned dielectric/metal nanostructures.[36] However, CR-AFM can be sensitive to the underlying substrate for few nanometers thick films and finite element modeling (FEM) can be required to extract thin film mechanical properties from the CR-AFM data.[37]

Two noncontact techniques that have recently demonstrated the potential to meet the above requirements are Brillouin light scattering (BLS)[38,39] and picosecond laser ultrasonics (PLU).[40–42] Both techniques effectively seek to determine the acoustic sound velocity of a material and then utilize equations relating sound velocity to elastic constants to determine engineering mechanical properties such as Young's modulus (E) and Poisson's ratio (ν).The former technique (BLS) relies on the detection of inelastically scattered light whereas the latter (PLU) relies on monitoring changes in surface reflectivity induced by an optically generated strain wave. Both techniques are noncontact (ideally nondestructive) optical techniques with limited substrate effects but have sufficient sensitivity to investigate films that approach 100 nm in thickness.[43,44] The applicability of both techniques for determining thin film elastic constants is also supported by previous observations of strong correlations between sound velocity and elastic constants for both porous and nonporous ceramic materials.[45,46]

BLS in particular has been demonstrated capable of determining the elastic constants for nm thick few layer graphene films[47] and patterned photoresist nanostructures.[48] Unfortunately, BLS experiments can be quite time consuming due to the need to perform multiple measurements at different scattering angles to determine the full set of elastic constants C_{ij} necessary to calculate both E and ν.[38,39] In contrast, PLU measurements are typically performed using a fixed optical alignment and are less time consuming.[49] However, the fixed alignment of PLU measurements allows only one elastic constant to be determined and engineering constants such as Young's modulus can only be determined via assuming a value for Poisson's ratio.[14]

Previous reports of BLS and PLU investigations of low-k materials have been primarily for nonporous dielectrics and direct comparisons of BLS and PLU have focused primarily on the BLS technique with minimal details regarding the PLU measurements.[50,51] In this report, both BLS and PLU are utilized to determine the mechanical properties of low-k dielectrics of differing porosity and composition with an emphasis on the PLU technique and comparison of PLS results to BLS. Two different approaches to PLU are specifically illustrated. In one case, a pump laser is utilized to launch an acoustic pulse into a thin film via thermal strain generated at the film/substrate interface. In the other case, an acoustic pulse is initiated in the surface of a metal coating deposited on top of the low-k dielectric. It is demonstrated that the values of Young's modulus determined by both PLU methods are in good agreement with BLS and that both BLS and PLU yield values that are comparable to nanoindentation measurements of identical films. It is also observed that while being a noncontact technique, the high energy laser typically utilized in PLU can significantly modify the properties of nanoporous low-k dielectrics in certain instances and can require careful PLU experimental design and setup.

2 Experimental

2.1 *Low-k Dielectric Deposition*

All the low-k dielectric materials investigated in this study were deposited on 300 mm diameter (100) Si substrates using a high volume manufacturing plasma enhanced chemical vapor deposition (PECVD) tool utilized in the fabrication of 32 nm low-k/Cu interconnects. The details of the PECVD film deposition have been provided previously.[11,43,51] Briefly, the precursors utilized consisted of various combinations of organosilanes, alkoxysilanes, and organic pore builders

(i.e., porogen) diluted in H_2, He, O_2, and other oxidizing gases. The nonporous films were deposited at temperatures on the order of 400°C, while the porous films were deposited at lower temperatures of 200 to 300°C to better facilitate incorporation of the porogen in the as deposited film. The porous films were given post deposition either an electron beam or UV cure at temperatures on the order of 400°C in order to remove the porogen and produce a porous film with improved mechanical properties.[52] All low-k dielectric materials investigated were characterized in either the as deposited or final cured state.

Film thickness and refractive index (RI) were determined using spectroscopic ellipsometry, and film mass density (needed for both BLS and PLU) was determined using x-ray reflectivity (XRR) as previously described.[53] The dielectric constant of the low-k films was determined by capacitance-voltage measurements using a Hg prober,[54] and the atomic composition was determined via combined Rutherford backscattering and nuclear reaction analysis.[55,56] The porosity was determined using an ellipsometric porosimetry technique.[43] Intrinsic film stress was determined using Stoney's formula and measurements of the change in the radius of curvature for the Si substrate before and after a-SiOC:H deposition.[53]

Table 1 summarizes some of the key material properties for the nonporous and porous a-SiOC:H dielectric materials investigated in this study including film composition, dielectric constant, RI, mass density, porosity, and intrinsic film stress. As can be seen, the a-SiOC:H materials examined span a range of k values that are representative of a-SiOC:H materials currently utilized or being considered for future low-k ILD applications. All films exhibit a relatively small tensile stress of 10 to 65 MPa that is expected to have a minimal influence on the BLS and PLU measurements. The a-SiOC:H films were all confirmed to be amorphous and isotropic via additional x-ray diffraction measurements previously described.[57]

2.2 *BLS*

Similar to Raman spectroscopy, BLS relies on detecting inelastic scattering events for light scattered from the surfaces of materials. Broadly, the two differ in the frequency of the detected scattering events with Raman spectroscopy detecting longitudinal and transverse optical modes and BLS recording similar low frequency acoustic modes.[58] For thin film geometries, standing acoustic modes with wave-vector components perpendicular to the film surface are quantized (m) and their frequency is related to the film thickness (h) and the elastic constants of the material.[51,52] The longitudinal- and transverse-standing mode (LSM and TSM) frequencies (f) can be described according to the relation

$$f = (2\ m + 1)V/4\ h, \tag{1}$$

where V is the corresponding acoustic wave velocity in the material. As can be seen, f is directly proportional to V and inversely proportional to the film thickness. Thus as film thickness decreases, the LSM and TSM frequencies become larger and more shifted from the elastic scattering peak and are thus easier to detect; although this advantage may be tempered by the reduced scattering volume and BLS intensity that occurs with reductions in h.[59]

Table 1 Summary of properties for PECVD low-k a-SiOC:H thin films investigated in this study. RI = refractive index at 673 nm.

Film	k (±0.1)	RI (±0.001)	Density (g/cm^3)	Porosity	Stress (MPa)
a-$SiO_{1.2}C_{0.9}$:H	3.05	1.43	1.35 ± 0.1	0	50 ± 5
a-$SiO_{0.87}C_{1.8}$:H	2.65	1.63	1.1 ± 0.1	12%	65 ± 5
a-$SiO_{1.15}C_{0.5}$:H	2.3	1.33	0.9 ± 0.1	33.5%	40 ± 5
a-$Si_{0.15}O_{0.09}C_{0.75}$:H	3.1	1.68	1.1 ± 0.1	2%	10 ± 5
a-$Si_{0.1}O_{0.14}C_{0.76}$:H	2.8	1.58	1.0 ± 0.1	12%	50 ± 5

The elastic constants of the material (C_{ii}) ($i = 1, 4$) are related to the mode frequencies from Eq. (1) as

$$C_{11} = 16h^2 f_L^2 \rho, \qquad C_{44} = 16h^2 f_T^2 \rho, \tag{2}$$

where ρ is the mass density of the film and f_L, f_T are the respective measured LSM and TSM mode frequencies. Poisson's ratio (ν) can then be computed using these C_{ii} values according to the relation

$$\nu = C_{12}/(C_{11} + C_{12}), \tag{3}$$

where C_{12} from the conditions of isotropy that require $C_{12} = (C_{11} - C_{44})/2$.[50] Young's modulus ($E$) can be similarly calculated according to

$$E = (1 + \nu)(1 - 2\nu)C_{12}/\nu, \tag{4}$$

where ν and C_{12} follow from the above relations and same assumptions of isotropy.[50]

For this study, the BLS measurements were performed in backscattering geometry at ambient temperature using approximately 70 mW p-polarized (=514.5 nm) radiation with the in-plane wave vector parallel to the (100) plane of the Si substrate. The scattering angle θ, measured from the film normal, was adjusted in 5 deg steps from 0 deg to 60 deg enabling the dispersion of the modes to be studied. To independently determine both C_{11} and C_{44}, longitudinal and transverse standing modes (LSM and TSM, respectively) must be detected close to the film normal. In backscattering, the LSM and TSM standing modes manifest at small scattering angles ($\theta < 10$ deg), while at higher angles the evolution of additional dispersive traveling waves was evident in the spectra.[50,51] The emergence of additional modes and their frequency variations with θ provide further constraints on the measured material elastic constants. For BLS, the film thicknesses ranged between 100 to 200 nm. For films thicker than 200 nm, the lower order TSM and LSM standing modes could not be observed due to overlap with the large elastic scattering peak.

2.3 *PLU*

PLU is a pump-probe technique that relies on a pump pulse from a laser to initiate a thermal strain wave in the film of interest and a time delayed beam from the same laser to probe and monitor changes in surface reflectivity induced by the propagation of the strain wave.[40,41] For films transparent to the wavelength of the pump laser, the strain wave can be generated directly via relying on optical absorption and heating at the film/substrate interface, or via using a thin opaque acousto-optic transducer metal layer[49] placed either at the film substrate interface[60–62] or on top of the film of interest.[14,49] In the first case, absorption at the film/substrate interface creates a thermal expansion strain that launches an acoustic pulse into both the film and substrate. As this acoustic pulse propagates through the film, the optical properties of the film are altered slightly due to the acousto-optic effect and a small amount of light is reflected by the acoustic pulse. Interference between the light reflected by the acoustic pulse and the rest of the film creates an oscillation in the change in reflectivity (ΔR) with a period of τ_{int}.[49] The period of oscillation is related to the longitudinal sound velocity (V_L) according to the relation

$$\tau_{\text{int}} = \lambda/2nV_L \cos(\theta), \tag{5}$$

where λ is the wavelength of the probe laser, n is the RI of the thin film at λ, and θ is the angle of incidence of the probe laser. As $V_L = hf_L$, C_{11} can be directly calculated using Eq. (2) above by measuring τ_{int} in the PLU experiment and determining n from other optical measurements such as spectroscopic ellipsometry. If a value of Poisson's ratio is assumed, C_{12} and in turn Young's modulus can be calculated according to Eqs. (3) and (4) above.[14]

For the case where a metal acousto-optic transducer coating is utilized, the absorption of the pump laser pulse by the surface of the metal film creates a similar thermal expansion strain that launches an acoustic pulse into the metal film that propagates down to the interface between the metal and the transparent film. Part of the acoustic pulse is reflected back into the metal and part

continues into the transparent film. A portion of the acoustic pulse propagating in the film will eventually reflect back at the film/substrate interface. The net result is that a time versus ΔR spectrum will have similar oscillatory components as described above.[49] The oscillations arising from acoustic pulses reflecting back and forth exclusively in the metal film decay quickly after short time delays whereas the oscillations arising from acoustic pulses traveling back and forth in the underlying transparent film will be observed at longer time delays. It should be noted that for both PLU setups an acoustic pulse does propagate in the substrate as well. For the Si substrates utilized in this study, this creates near time zero an additional small oscillatory signal of 4 ps due to the high sound velocity of the crystalline substrate.

It should also be noted that while film thickness h does not directly enter into Eq. (5), it is an important consideration in that the film needs to be thick enough to observe the oscillations in ΔR within the time resolution of the experiment. For typical low-k materials, film thicknesses of 500 to 1,000 nm are typically more than sufficient for this purpose. However as film thickness decreases, fewer periods of the ΔR oscillation will be observed and there will be a critical thickness below which the full period can no longer be resolved. This topic will be discussed further later for the specific films in this study. For the PLU measurements, the film thickness was intentionally skewed from 500 down to 100 nm to assess the impact of film thickness and determine the minimum thickness for ideal PLU measurements.

In this investigation, both PLU approaches were applied to the nanoporous low-k dielectrics described in Table 1. Short pulses (less than 100 fs) from a Ti:sapphire oscillator operating at a repetition rate of 76 MHz were utilized for both the pump and probe. The pulsed optical beam is split into pump and probe beams and then both beams are focused onto the same ~10 to 40 μm diameter spot on the sample. Before being focused onto the pump spot, the probe beam is directed to a translation stage which allows us to delay the arrival of probe pulses with respect to the pump pulses by as much as several nanoseconds with subpicosecond resolution. For the PLU experiments where an acousto-optic metal transducer over layer was utilized, 40 to 80 nm of aluminum was deposited on top of the low-k film to be studied via electron beam evaporation.[14] For PLU experiments where no metal coating transducer was utilized, the sapphire output was frequency doubled to 400 nm to increase absorption at the film/substrate interface as has been previously described by Antonelli.[49]

2.4 *Nanoindentation*

Nanoindentation experiments were performed on thicker 1 to 2 micrometer films using a Hysitron Triboindenter and a cube corner diamond tip with a load range of 5 to 30 mN.[53,63] Each sample was analyzed using fifteen indents. Samples were loaded in a continuous stiffness mode. The modulus was calculated using a shallow contact depth range of <150 nm to avoid substrate interaction effects in the 1 micrometer thick samples investigated.

The authors note that some variations in mechanical properties with film thickness is possible for the low-k dielectric films investigated in this study due to differences in both deposition times and UV/ebeam cure times.[64] However, these differences are expected to be <0.5 GPa and as we will show later are comparatively insignificant relative to the large substrate effects observed in the nanoindentation measurements.

3 Results

3.1 *BLS*

Figure 1 shows a typical series of BLS spectra collected at different scattering angles (θ) from a 150 nm thick sample of the k = 3.05 SiOC:H dielectric. Various resonances in the spectra can be detected and that shift with scattering angle. The BLS peak intensities, their frequencies, and the manner in which these resonances shift with θ, allows the identification of the LSM or TSM acoustic modes.[59]

The observed principle [$m = 0$ in Eq. (1)] and higher order ($m = 1, 2, \ldots$) LSM and TSM harmonics in combination with Eq. (1) enable the associated material acoustic wave velocity to

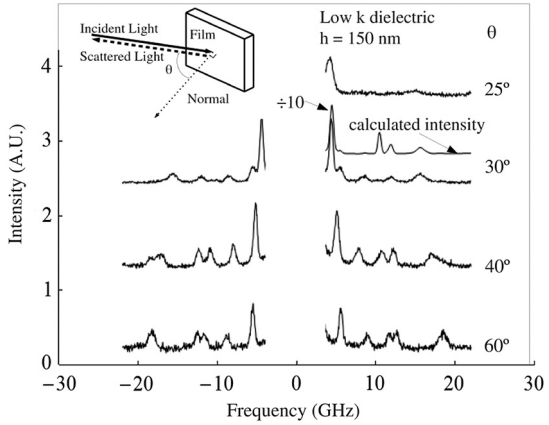

Fig. 1 Example BLS spectra collected from a 150 nm thick, k = 3.05 SiOC:H dielectric. Spectra were collected at various scattering angles (θ).

be determined. If the mass density of the material is known independently, the C_{ij} elastic constants, Poisson's ratio and Young's modulus can also be determined. Table 2 summarizes the Young's modulus determined for the above a-SiOC:H material as well as the additional porous low-k a-SiOC:H dielectrics investigated in this study.[43,50,51] The BLS numbers are compared against NI measurements performed on identical materials. As is evident, the two techniques provide similar results with the BLS numbers being slightly lower than the NI results for both films. This is consistent with acoustic methods in general reporting slightly lower values for Young's modulus relative to NI techniques. This has been presumed to be due to substrate and indentation hardening effects in the NI measurements.[49]

3.2 *PLU*

PLU data ($\Delta R/R$ versus time delay) collected without a metal acousto-optic transducer coating are illustrated in Fig. 2 for the same k = 3.05 a-SiOC:H dielectric utilized to illustrate the BLS measurements in Fig. 1. As mentioned previously, the high frequency (4 ps) oscillations in $\Delta R/R$ near time zero are due to acoustic pulses propagating in the Si substrate. At longer time delays, a lower frequency oscillation with a period of 56 ps can be observed that is due to the acoustic pulse created at the film/substrate interface propagating back and forth in the low-k dielectric. PLU data collected for the same film with a metal acousto-optic transducer is presented in Fig. 3. In this case, the spike in reflectivity change near time zero is the electronic response of the thin Al film as it absorbs the pump pulse. This absorption causes a rapid thermal expansion that launches the picosecond ultrasonic pulse. The oscillation in $\Delta R/R$ immediately following time zero is caused by the ultrasonic pulse as it bounces back and forth in the Al film. The revival of these oscillations after 300 ps gives the time for an

Table 2 Summary of Young's modulus values determined by NI, BLS, and PLU for the PECVD low-k a-SiOC:H thin films investigated in this study. PLU-D indicates PLU without a metal transducer, and PLU-M with a metal transducer.

Film	NI (GPa)	BLS (GPa)	PLU-D (GPa)	PLU-M (GPa)
a-$SiO_{1.2}C_{0.9}$:H	11.8 ± 1[50]	8.4 ± 1.6[50]	8.9 ± 0.9	8.8 ± 0.9
a-$SiO_{0.87}C_{1.8}$:H	9.7 ± 0.9[51]	5.7 ± 1.1[51]	5.1 ± 0.5	4.7 ± 0.5
a-$SiO_{1.15}C_{0.5}$:H	5.1 ± 0.5[43]	2.6 ± 0.4[43]	3.4 ± 0.3	2.55 ± 0.3
a-$Si_{0.15}O_{0.09}C_{0.75}$:H	6.3 ± 0.2[51]	4.8 ± 0.7[51]	5.9 ± 0.6	6.8 ± 0.6
a-$Si_{0.1}O_{0.14}C_{0.76}$:H	5.6 ± 0.4[51]	6.8 ± 0.9[51]	3.8 ± 0.7	—[a]

[a]Sample not measured due to high acoustic attenuation and mismatch between Al and sample.

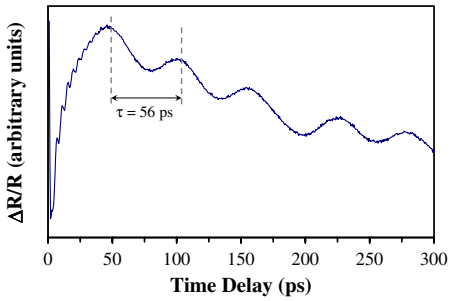

Fig. 2 PLU spectrum for the k = 3.05 SiOC:H dielectric acquired without a metal transducer.

ultrasonic pulse to travel one round trip through the a-SiOC:H layer. It should be noted that the period of these oscillations (about 20 ps) is determined by the thickness and sound velocity of the Al transducer and is different from the period illustrated in Fig. 2 for measurements without the transducer.

Young's modulus values were computed using Eqs. (3) to (5) for all five films from both sets of PLU data. These data are reported in Table 2 along with the NI and BLS data. Without prior knowledge of the Poisson's ratio determined by BLS, this value was assumed to be $\nu = 0.25$ for all films. The value of Poisson's ratio determined from the previously mentioned BLS measurements was 0.22 to 0.27 and validates $\nu = 0.25$ to be a reasonable assumption for the PLU measurments.[51] As can be seen, the PLU results are in strong agreement with BLS and show the same offset relative to the NI measurements.

To test the thickness limitation of the PLU technique for low-k dielectrics, additional PLU measurements were performed on some of the low-k dielectrics at 300 and 100 nm thickness. In Fig. 4, the PLU spectra collected without a metal transducer coating are presented for the k = 3.05 a-SiOC:H dielectric at 500, 300, and 100 nm thicknesses. An oscillatory signal is clearly observed at 500 and 300 nm. However at 100 nm, an oscillatory signal is no longer observed. This is attributed to the transit time for the acoustic strain pulse to propagate up and down the film being shorter than the resolution of the PLU experiment for this film. A similar thickness dependence was observed for all the other a-SiOC:H films listed in Table 1. This is in contrast to the BLS measurements where successful measurements have been previously demonstrated at 100 to 150 nm thicknesses.[43,51]

As noted in a previous publication,[51] an additional concern for PLU measurements of low-k dielectrics is modification (i.e., "burning") of the material by the intense pump/probe laser. For much thicker (1 to 2 micrometer) versions of the films in Table 1, pump/probe laser trace marks could be visibly observed on the surface of all the porous films measured without a metal transducer coating. However, such burn marks were less obvious to the naked eye at <500 nm. To test the influence of the PLU measurement on the resulting measured properties, the PLU measurements were repeated six times on two different 500 nm thick a-SiOC:H films. As shown in Fig. 5, no change in Young's modulus was observed for the k = 3.05 a-SiOC:H

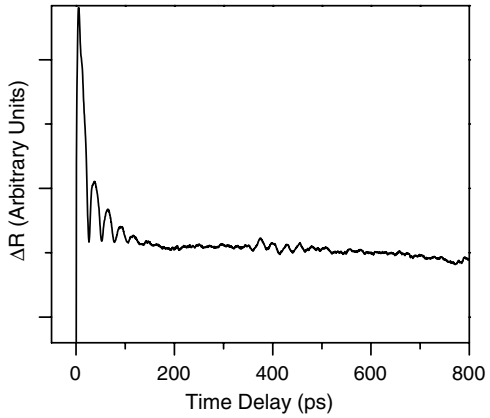

Fig. 3 PLU spectra for k = 3.05 a-SiOC:H collected with an Al metal transducer coating.

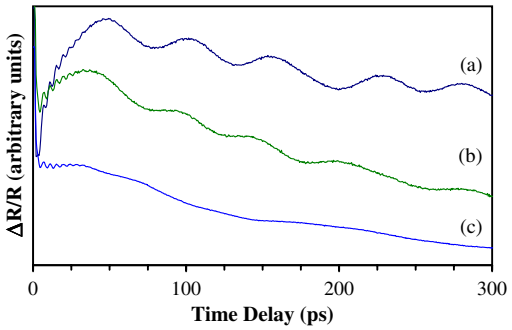

Fig. 4 PLU spectra for k = 3.05 a-SiOC:H at (a) 500 nm, (b) 300 nm, and (c) 100 nm.

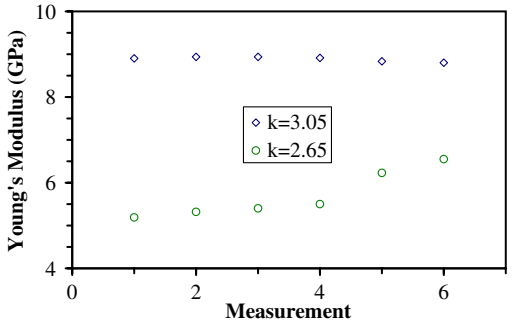

Fig. 5 PLU Young's modulus as a function of number of measurements for a 500 nm thick nonporous and porous a-SiOC:H low-k dielectric.

dielectric after six measurements consistent with the lack of any observed burning for this film. In contrast, a slight increase in Young's modulus of about 5% was observed for the k = 2.65 a-SiOC:H dielectric after a few measurements and increased by 25% after the sixth measurement. This is consistent with visual observations of thicker versions of this particular film being more sensitive to burning by the pump/probe laser. It should also be noted that while burning was not observed for the PLU measurements using a metal transducer coating, this may not preclude such adverse thermal effects from being a concern for these types of PLU measurements. In fact, it could explain the lack of an oscillatory signal for the k = 2.8 SiOC:H film that was previously attributed to acoustic mismatch between the transducer and low-k film.[14]

4 Discussion

The two primary attractive features of BLS to characterize the mechanical properties of materials are that the method is: 1. nondestructive, requiring no special specimen preparation, and 2. capable of determining all independent elastic constants, i.e., Young's modulus and Poisson's ratio of bulk supported and freestanding films.[59,65,66] Moreover, the technique has been extended to ultra-thin films from 200 nm down to a few nm.[47] BLS takes advantage of the detection of different acoustic modes of submicrometer wavelengths that are naturally present in the medium and are selected by the scattering geometry, thereby eliminating the need for acoustic transducers. The detected excitations include longitudinal, transverse and shear horizontal bulk modes as well as the Rayleigh surface and pseudosurface modes. In the case of thin films as illustrated above, pure LSM and TSM harmonics, which are acoustic waves trapped within the film that reflect back and forth along the normal to the film surface, are respectively sensitive to C_{11} and C_{44}. The transition of these standing modes into propagating waves along different crystallographic directions provides further verification of the elastic constants as well as a complete characterization of the elastic properties. The drawbacks to BLS measurements of low-k dielectrics is the time needed to acquire and interpret data collected at multiple scattering angles, and the sophisticated optical setup needed to detect the Brillouin scattering peaks in the presence of an elastic scattering peak many orders of magnitude more intense.

While also requiring a sophisticated optical setup, the fixed optical geometry and reliance on detecting changes in surface reflectivity utilized in PLU measurements allows faster measurements and addresses some of the drawbacks associated with BLS. However, PLU measurements provide only one elastic constant (C_{11}) and assumptions regarding the other elastic constants (primarily Poisson's ratio) are needed to determine Young's modulus. These limitations could potentially be addressed via performing PLU at multiple scattering angles as demonstrated by Lomonosov,[62] but would also significantly decrease the throughput of the technique. As shown above, PLU is also potentially limited to characterizing low-k dielectric films >100 nm in thickness and sample burning by the pump/probe laser can also be a concern.

BLS and PLU both present several advantages over NI that have already been discussed previously in the introduction. While both BLS and PLU have their drawbacks as noted above, the two techniques are complementary to one another. Both have sufficient sensitivity to determine the mechanical properties of low-k dielectric films at thicknesses of 100 to 200 nm. The ability of PLU to determine only one elastic constant can be addressed by BLS measurements of the same film to determine the full set of elastic constants and thus enable calculation of Young's modulus via PLU without having to assume a value for Poisson's ratio. This in turn allows the limited throughput of BLS measurements to be overcome via PLU measurements that are more amenable to automation and process control monitoring. The potential for BLS to be extended to films as thin as a few nm, likewise can address the thickness limitations of PLU and potentially suggest refinements to the PLU experimental setup to probe ≤100 nm thick films. Thus, BLS and PLU combined have the capability to complement one another while providing a robust characterization of the mechanical properties of few nm thick films and patterned nanostructures.

As mentioned above, PLU does have the added complication of potentially altering/burning the material during the pump/probe measurement, particularly for porous low-k dielectrics. This challenge may be partially mitigated by utilizing a metal transducer top coating to prevent significant absorption by the low-k dielectric or through better selection of the laser wavelength. For the latter, we do note that optical absorption measurements and reflection electron energy loss spectroscopy measurements have shown that the band gap for low-k dielectric materials are typically quite large at >8.0 eV.[67,68] However, significant absorption at lower photon energies/higher wavelengths is observed for porous low-k dielectrics and is attributed to residual porogen residues not completely removed from the film during electron beam or UV curing.[68–70] This could explain the lack of any observed burning in our PLU measurements on nonporous (i.e., nonporogen) films and burning for the porous films. It likewise could explain the lack of burning in other PLU investigations of low-k dielectrics where longer wavelength 800 nm pump/probe lasers were utilized.[60–62] We should also note the potential for burning of the low-k dielectric by the laser in BLS measurements. While a slightly longer wavelength laser (514.5 nm) was utilized and signs of burning were not observed, we cannot currently completely rule out this effect for BLS measurements of porous low-k dielectrics and this will be the subject of future BLS investigations of low-k materials.

An additional advantage of PLU recently demonstrated for the examination of low-k dielectrics is the ability to perform a depth profile of the sound velocity/elastic constants across the thickness of the film.[61,62] For UV cured low-k dielectrics in particular, constructive/deconstructive interference of the UV light in the film during curing can result in portions of the film being comparatively over or under cured. Lomonosov and Mechri have shown that this can result in asymmetries in the observed period in PLU spectra for UV cured porous low-k films.[61,62] They have further shown that these asymmetries can be modeled and exploited to determine the longitudinal sound velocity as a function of film thickness. For an 800 nm thick, k = 2.5, 25% porous UV cured low-k dielectric, they demonstrated that the longitudinal sound velocity and mass density can vary by up to 10% to 20% across the thickness of the film and accordingly Young's modulus should vary by a similar amount.[62]

In this regard, we do note that similar asymmetries were observed in the PLU spectra for only one of the porous low-k dielectrics examined in this study. As shown in Fig. 6, a gradual increase in peak-to-peak period was observed for our k = 2.8 SiOC:H dielectric film. For this particular film, Young's modulus was determined using only the first observed period. Using the average of all the observed periods would increase the error by approximately 10% and is reflected in the

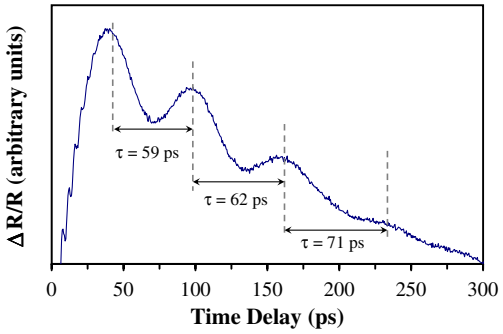

Fig. 6 PLU spectrum for a k = 2.8, 12% porous SiOC:H dielectric.

larger error bars for this sample. As picosecond ultrasonics is accurate to within less than a picosecond, the uncertainty of ±10% in the other measurements is primarily a function of both the uncertainty of the film mass density (typically 5% to 10% for XRR) and the RI/film thickness (typically 1% to 3% for ellipsometry).[15,56]

5 Summary and Conclusions

BLS and PLU have both been utilized to investigate the mechanical properties of low-k dielectrics representative of materials commonly used in the semiconductor industry for fabrication of low-k/Cu interconnect structures. The values of Young's modulus determined by both techniques were compared against each other and against values determined by nanoindentation (the industry standard technique). The values evaluated by all three techniques were consistent and comparable with one another. While both BLS and PLU present unique advantages and disadvantages, the two techniques combined show promise for extension to measuring the mechanical properties of low-k dielectrics at 100 to 200 nm thickness.

Acknowledgments

B. Daly supervised and analyzed PLU measurements performed by Donald Hondongwa, Lauren Olasov, Joseph Andrade, and Bryan Rachmilowitz during their undergraduate studies at Vassar College. R. Sooryakumar supervised BLS measurements and analysis performed by S. Bailey during research for his PhD. S. King supervised and analyzed additional PLU measurements performed by B. Colvin, J. Kelly, and K. Scharfenberger at Intel Corporation. S. King also coordinated and facilitated nanoindentation measurements performed by Dr. Jessica Xu and Liza Ross at Intel Corporation. B. Daly, S. Bailey, R. Sooryakumar, and S. King all contributed equally to writing the manuscript and S. King coordinated the organization of the final article. The authors would also like to acknowledge the invaluable guidance and discussions with Drs. Andy Antonelli, Andre Miller, and Rubina Sultan, and the support and encouragement from Drs. B. Tufts, J. Maiz, and B. Boyanov of Intel Corporation during the course of this research. Support from the Institute for Materials Research at The Ohio State University is also acknowledged.

References

1. C. Auth et al., "45 nm high-k + metal gate strain-enhanced transistors," in *IEEE Symp. on VLSI Technology*, pp 128–129, IEEE, New York (2008).
2. E. Karl et al., "A 4.6 GHz 162 Mb SRAM design in 22 nm tri-gate CMOS technology with integrated active VMIN-enhancing assist circuitry," in *IEEE International Solid-State Circuits Conference Digest of Technical Papers*, pp. 230–232, IEEE, New York (2012).
3. G. Moore, "Cramming more components onto integrated circuits," *Proc. IEEE* **86**(1), 82–85 (1998), http://dx.doi.org/10.1109/JPROC.1998.658762.
4. K. Kuhn, "Moore's crystal ball: device physics and technology past the 15 nm generation," *Microelectron. Eng.* **88**(7), 1044–1049 (2011), http://dx.doi.org/10.1016/j.mee.2011.03.163.
5. M. Bohr, "Interconnect scaling–the real limiter to high performance ULSI," in *IEEE International Electron Devices Meeting (IEDM'95)*, pp. 241–244, IEEE, New York (1995).

6. S. Tyagi et al., "A 130 nm generation logic technology featuring 70 nm transistors dual Vt transistors and 6 layers of Cu interconnects," in *IEEE International Electron Devices Meeting (IEDM'00)*, pp. 567–570, IEEE, New York (2000).
7. Y. Kim et al., "Infrared spectroscopy study of low-dielectric-constant fluorine-incorporated and carbon-incorporated silicon oxide films," *J. Appl. Phys.* **90**(7), 3367–3370 (2001), http://dx.doi.org/10.1063/1.1402152.
8. S. Yang et al., "A high performance 180 nm generation logic technology," in *IEEE International Electron Devices Meeting (IEDM'98)*, pp. 197–200, IEEE, New York (1998).
9. K. Maex et al., "Low dielectric constant materials for microelectronics," *J. Appl. Phys.* **93**(11), 8793–8841 (2003), http://dx.doi.org/10.1063/1.1567460.
10. W. Volksen, R. Miller, and G. Dubois, "Low dielectric constant materials," *Chem. Rev.* **110**(1), 56–110 (2010), http://dx.doi.org/10.1021/cr9002819.
11. E. Andideh et al., "Compositional effects on electrical and mechanical properties in carbon-doped oxide dielectric films: application of Fourier-transform infrared spectroscopy," *J. Vac. Sci. Technol. B* **22**(1), 196–201 (2004), http://dx.doi.org/10.1116/1.1640401.
12. C. Jan et al., "90 nm generation, 300 mm wafer low k ILD/Cu interconnect technology," in *IEEE 2003 International Interconnect Technology Conference*, pp. 15–17, IEEE, New York (2003).
13. S. King and J. Bielefeld, "Rigidity percolation in plasma enhanced chemical vapor deposited a-SiC:H thin films," *ECS Trans.* **33**(8), 185–194 (2010), http://dx.doi.org/10.1149/1.3484122.
14. D. Hondongwa et al., "Thermal conductivity and sound velocity measurements of plasma enhanced chemical vapor deposited a-SiC:H thin films," *Thin Solid Films* **519**(22), 7895–7898 (2011), http://dx.doi.org/10.1016/j.tsf.2011.05.014.
15. S. King and A. Antonelli, "Simple bond energy approach for non-destructive measurements of the fracture toughness of brittle materials," *Thin Solid Films* **515**(18), 7232–7241 (2007), http://dx.doi.org/10.1016/j.tsf.2007.02.106.
16. A. Volinsky, J. Vella, and W. Gerberich, "Fracture toughness, adhesion and mechanical properties of low-K dielectric thin films measured by nanoindentation," *Thin Solid Films* **429**(1–2), 201–210 (2003), http://dx.doi.org/10.1016/S0040-6090(03)00406-1.
17. M. Hussein and J. He, "Materials' impact on interconnect process technology and reliability," *IEEE Trans. Semi. Manf.* **18**(1), 69–85 (2005), http://dx.doi.org/10.1109/TSM.2004.841832.
18. S. King and J. Gradner, "Intrinsic stress fracture energy measurements for PECVD thin films in the SiOxCyNz:H system," *Microelectron. Rel.* **49**(7), 721–726 (2009), http://dx.doi.org/10.1016/j.microrel.2009.04.006.
19. G. Antonelli et al., "Synergistic combinations of dielectrics and metallization process technology to achieve 22 nm interconnect performance targets," *Microelectron. Eng.* **92**, 9–14 (2012), http://dx.doi.org/10.1016/j.mee.2011.04.035.
20. D. Gidley, H. Peng, and R. Vallery, "Positron annihilation as a method to characterize porous materials," *Ann. Rev. Mat. Res.* **36**, 48–79 (2006), http://dx.doi.org/10.1146/annurev.matsci.36.111904.135144.
21. K. Phani and S. Niyogi, "Young's modulus of porous brittle solids," *J. Mater. Sci.* **22**(1), 257–263 (1987), http://dx.doi.org/10.1007/BF01160581.
22. G. Antonelli et al., "Designing ultra-low-k dielectric materials for ease of patterning," *MRS Proc.*, Vol. 1249, pp. F04–F06, Cambridge University Press, New York (2010).
23. M. Garner et al., "Challenges for dielectric materials in future integrated circuit technologies," *Microelectron. Rel.* **45**(5–6), 919–924 (2005), http://dx.doi.org/10.1016/j.microrel.2004.11.053.
24. K. Mosig et al., "Integration challenges of porous ultra low-k spin-on dielectrics," *Microelectron. Eng.* **64**(1–4), 11–24 (2002), http://dx.doi.org/10.1016/S0167-9317(02)00767-0.
25. "Emerging research materials," The International Technology Roadmap for Semiconductors, Semiconductor Industry Association, San Jose, California, http://www.itrs.net/Links/2011ITRS/Home2011.htm (2011).
26. T. Frot et al., "Post porosity plasma protection: scaling of efficiency with porosity," *Adv. Funct. Mater.* **22**(14), 3043–3050 (2012), http://dx.doi.org/10.1002/adfm.v22.14.

27. H. Yoo et al., "Demonstration of a reliable high-performance and yielding air gap interconnect process," in *IEEE 2010 International Interconnect Technology Conference*, pp. 1–3, IEEE, New York (2010).
28. R. Brain et al., "Low-k interconnect stack with a novel self-aligned via patterning process for 32 nm high volume manufacturing," in *IEEE 2009 International Interconnect Technology Conference*, pp. 249–251, IEEE, New York (2009).
29. S. Nagao et al., "Achieving consistency of Young's modulus determination from nanoscale deformation of low-k films," *J. Appl. Phys.*, **105**(10), 106104 (2009), http://dx.doi.org/10.1063/1.3117526.
30. K. Yonekura et al., "Investigation of ash damage to ultralow-k inorganic materials," *J. Vac. Sci. Technol. B* **22**(2), 548–553 (2004), http://dx.doi.org/10.1116/1.1651111.
31. D. Hurley et al., "Nanoscale elastic-property measurements and mapping using atomic force acoustic microscopy methods," *Meas. Sci. Technol.* **16**(11), 2167–2172 (2005), http://dx.doi.org/10.1088/0957-0233/16/11/006.
32. G. Stan and W. Price, "Quantitative measurements of indentation moduli by atomic force acoustic microscopy using a dual reference method," *Rev. Sci. Inst.* **77**(10), 103707 (2006), http://dx.doi.org/10.1063/1.2360971.
33. G. Stan, S. King, and R. Cook, "Elastic modulus of low-k dielectric thin films measured by load-dependent contact-resonance atomic force microscopy," *J. Mater. Res.* **24**(9), 2960–2964 (2009), http://dx.doi.org/10.1557/jmr.2009.0357.
34. D. Hurley et al., "Anisotropic elastic properties of nanocrystalline nickel thin films," *J. Mater. Res.* **20**(5), 1186–1193 (2005), http://dx.doi.org/10.1557/JMR.2005.0146.
35. G. Stan et al., "Surface effects on the elastic modulus of Te nanowires," *Appl. Phys. Lett.* **92**(24), 241908 (2008), http://dx.doi.org/10.1063/1.2945285.
36. G. Stan, S. King, and R. Cook, "Nanoscale mapping of contact stiffness and damping by contact resonance atomic force microscopy," *Nanotechnol.* **23**(21), 215703 (2012), http://dx.doi.org/10.1088/0957-4484/23/21/215703.
37. D. Hurley, "Contact resonance force microscopy techniques for nanomechanical measurements," in *Applied Scanning Probe Methods XI, NanoScience and Technology*, B. Bhusan and H. Fuchs, Eds., p. 97, Springer, New York (2009).
38. G. Carlotti, L. Doucet, and M. Dupeux, "Comparative study of the elastic properties of silicate glass films grown by plasma enhanced chemical vapor deposition," *J. Vac. Sci. Technol. B* **14**(6), 3460–3464 (1996), http://dx.doi.org/10.1116/1.588780.
39. X. Jiang et al., "Mechanical properties of a-Si:H films studied by Brillouin scattering and nanoindenter," *J. Appl. Phys.* **67**(11), 6772–6778 (1990), http://dx.doi.org/10.1063/1.345064.
40. H. Grahn, H. Maris, and J. Tauc, "Picosecond ultrasonics," *IEEE J. Quant. Electron.* **25**(12), 2562–2569 (1989), http://dx.doi.org/10.1109/3.40643.
41. C. Thomsen et al., "Surface generation and detection of phonons by picosecond light pulses," *Phys. Rev. B* **34**(6), 4129–4138 (1986), http://dx.doi.org/10.1103/PhysRevB.34.4129.
42. H. Ogi et al., "Resonance acoustic-phonon spectroscopy for studying elasticity of thin films," *Appl. Phys. Lett.* **90**(19), 191906–191908 (2007), http://dx.doi.org/10.1063/1.2737819.
43. S. Bailey et al., "Mechanical properties of high porosity low-k dielectric nano-films determined by Brillouin light scattering," *J. Phys. D* **46**(4), 045308 (2013), http://dx.doi.org/10.1088/0022-3727/46/4/045308.
44. J. Bryner et al., "Characterization of Ta and TaN diffusion barriers beneath Cu layers using picosecond ultrasonics," *Ultrasonics* **44**(Suppl. 22), 1269–1275 (2006), http://dx.doi.org/10.1016/j.ultras.2006.05.097.
45. A. Wanner, "Elastic modulus measurements of extremely porous ceramic materials by ultrasonic phase spectroscopy," *Mat. Sci. Engr. A* **248**(1–2), 35–43 (1998), http://dx.doi.org/10.1016/S0921-5093(98)00524-3.
46. J. Gross, G. Reichenauer, and J. Fricke, "Mechanical properties of SiO2 aerogels," *J. Phys. D: Appl. Phys.* **21**(9), 1447–1451 (1988), http://dx.doi.org/10.1088/0022-3727/21/9/020.
47. Z. Wang et al., "Brillouin scattering study of low-frequency bulk acoustic phonons in multilayer graphene," *Carbon* **46**(15), 2133–2136 (2008), http://dx.doi.org/10.1016/j.carbon.2008.09.028.

48. R. Hartschuh et al., "Brillouin scattering studies of polymeric nanostructures," *J. Poly. Sci. B* **42**(6), 1106–1113 (2004), http://dx.doi.org/10.1002/(ISSN)1099-0488.
49. A. Antonelli et al., "Characterization of mechanical and thermal properties using ultrafast optical metrology," *MRS Bulletin* **31**(8), 607–613 (2006), http://dx.doi.org/10.1557/mrs2006.157.
50. A. Link et al., "Brillouin light scattering studies of the mechanical properties of ultrathin low-k dielectric films," *J. Appl. Phys.* **100**, 013507 (2006), http://dx.doi.org/10.1063/1.2209428.
51. W. Zhou et al., "Elastic properties of porous low-k dielectric nano-films," *J. Appl. Phys.* **110**(4), 043520 (2011), http://dx.doi.org/10.1063/1.3624583.
52. V. Jousseaume et al., "Comparison between e-beam and ultraviolet curing to perform porous a-SiOC:H," *J. Electrochem. Soc.* **154**(5), G103–G109 (2007), http://dx.doi.org/10.1149/1.2667980.
53. S. King et al., "Intrinsic stress effect on fracture toughness of plasma enhanced chemical vapor deposited SiNx:H films," *Thin Solid Films* **518**(17), 4898–4907 (2010), http://dx.doi.org/10.1016/j.tsf.2010.03.031.
54. S. King et al., "Film property requirements for hermetic low-k a-SiOxCyNz:H dielectric barriers," *ECS J. Solid State Sci. Technol.* **1**, N115–N122 (2012), http://dx.doi.org/10.1149/2.021206jss.
55. S. King et al., "Fourier transform infrared spectroscopy investigation of chemical bonding in low-k a-SiC:H thin films," *J. Non-Cryst. Sol.* **357**, 2970–2983 (2011), http://dx.doi.org/10.1016/j.jnoncrysol.2011.04.001.
56. S. King et al., "Mass and bond density measurements for PECVD a-SiC:H thin films using Fourier transform-infrared spectroscopy," *J. Non-Cryst. Sol.* **357**(21), 3602–3615 (2011), http://dx.doi.org/10.1016/j.jnoncrysol.2011.07.004.
57. T. Phung, D. Johnson, and G. Antonelli, "A detailed experimental and analytical study of thermal expansion of dielectric thin films on Si by X-ray reflectivity," *J. Appl. Phys.* **100**(6), 064317 (2006), http://dx.doi.org/10.1063/1.2353283.
58. A. Bassi et al., "Inelastic light scattering: a multiscale characterization approach to vibrational, structural and thermo-mechanical properties of nanostructured materials," *Appl. Surf. Sci.* **226**(1–3), 271–281 (2004), http://dx.doi.org/10.1016/j.apsusc.2003.11.041.
59. S. King et al., "Advances in metrology for the determination of Young's modulus for low-k dielectric thin films," *Proc. SPIE* **8466**, 84660A (2012), http://dx.doi.org/10.1117/12.930482.
60. C. Mechri et al., "Evaluation of elastic properties of nanoporous silicon oxide thin films by picosecond laser ultrasonics," *Eur. Phys. J.* **153**(1), 211–213 (2008), http://dx.doi.org/10.1140/epjst/e2008-00430-8.
61. C. Mechri et al., "Depth-profiling of elastic inhomogeneities in transparent nanoporous low-k materials by picosecond ultrasonic interferometry," *Appl. Phys. Lett.* **95**(9), 091907 (2009), http://dx.doi.org/10.1063/1.3220063.
62. A. Lomonosov et al., "Nanoscale noncontact subsurface investigations of mechanical and optical properties of nanoporous low-k materials thin film," *ACS Nano* **6**(2), 1410–1415 (2012), http://dx.doi.org/10.1021/nn204210u.
63. G. Kloster et al., "Porosity effects on low-k dielectric film strength and interfacial adhesion," in *IEEE 2002 International Interconnect Technology Conference*, pp. 242–244, IEEE, New York (2002).
64. Y. Shioya et al., "Effect of UV anneal on plasma CVD low-k film," *J. Non-Cryst. Sol.* **354**(26), 2973–2982 (2008), http://dx.doi.org/10.1016/j.jnoncrysol.2007.12.011.
65. R. Bandhu et al., "Acoustic vibrations in free-standing double layer membranes," *Phys. Rev. B* **70**(7), 75409 (2004), http://dx.doi.org/10.1103/PhysRevB.70.075409.
66. G. Greaves et al., "Poisson's ratio and modern materials," *Nat. Mater.* **10**, 823–837 (2011), http://dx.doi.org/10.1038/nmat3134.
67. J. Lauer et al., "Charge trapping within UV and vacuum UV irradiated low-k porous organosilicate dielectrics," *J. Electrochem. Soc.* **157**(8), G177–G182 (2010), http://dx.doi.org/10.1149/1.3435285.

68. S. King, B. French, and E. Mays, "Detection of defect states in low-k dielectrics using reflection electron energy loss spectroscopy," *J. Appl. Phys.* **113**(4), 44109 (2013), http://dx.doi.org/10.1063/1.4788980.
69. P. Marsik et al., "Porogen residues detection in optical properties of low-k dielectrics cured by ultraviolet radiation," *Thin Solid Films* **518**(15), 4266–4272 (2010), http://dx.doi.org/10.1016/j.tsf.2009.12.110.
70. A. Urbanowicz et al., "Effect of UV wavelength on the hardening process of porogen-containing and porogen-free ultralow-k plasma-enhanced chemical vapor deposition dielectrics," *J. Vac. Sci. Technol. B* **29**(3), 032201 (2011), http://dx.doi.org/10.1116/1.3572063.

Brian C. Daly is associate professor of physics at Vassar College in Poughkeepsie, New York. He received a PhD in physics from Brown University in 2003. His experimental interests include time-resolved ultrafast studies of phonon transport in crystals, thin films, and nanostructures.

Sheldon T. Bailey received a BS degree in physics from Pennsylvania State University, University Park, The Behrend College, Erie, Pennsylvania, in 2005. He is currently working toward a PhD degree in physics at The Ohio State University, Columbus. His research is related to light-scattering studies to probe the elastic properties of laminar structures and membranes.

Ratnasingham Sooryakumar received MS and PhD degrees in physics from the University of Illinois, Champaign-Urbana in 1976 and 1980, respectively. Following his PhD degree, he was the recipient of an Alexander von Humboldt Fellowship to conduct research at the Max Planck Institute in Stuttgart, Germany, where he remained until 1983. After spending a year at AT&T Bell Laboratories, in Holmdel, New Jersey, USA, he joined the Department of Physics at The Ohio State University in 1984 where he is currently a professor of physics. His research interests have largely been in the application of Raman and Brillouin scattering to probe the electronic, magnetic and elastic properties of a broad class of condensed matter and biological systems. In addition, his current research activities include development of mobile magnetic tweezers for biological and engineering applications at the micro- and nanoscales. He is a fellow of the American Physical Society.

Sean W. King is a senior technical contributor within Intel Corporation's Logic Technology Development Division. Since joining Intel in 1997, He has held a variety of technical positions in the development of Intel's micro/nano-electronic technologies. He is currently leading the development and integration of new chemically vapor deposited low dielectric constant materials for Intel's 12 nm technology. He also serves as a faculty member within Intel's College of Engineering and as an adjunct professor within the Electrical and Computer Engineering Department at Georgia Tech. His additional research interests include nanometer scale diffusion barriers, III-V nitride semiconductors, thin film mechanics, and advanced metrologies for electrical-optical-mechanical property characterization of dielectric and semiconducting materials. He holds a BS degree in materials engineering from Virginia Tech and a PhD in materials science and engineering from North Carolina State University.